

Figure 4. Views of the three rotational isomers of the Δ - β_2 -[Co(asp)(N₄)]⁺ ion through the bond (top) and in perspective (bottom).

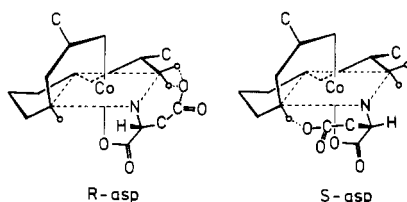


Figure 5. Possible structures of the Δ - β_2 -[Co(asp)(2(*S*),10(*S*)-Me₂-2,3,2-tet)]⁺ ion.

two outer five-membered chelate rings are fixed to the δ -(1el) conformation, and higher stereoselectivities were observed in these systems. Therefore, it is an important factor for the high stereoselectivity in the Δ -[Co(asp or asn)(N₄)]ⁿ⁺ systems that the conformations of the two outer five-membered chelate rings are fixed rigidly to the $\delta\delta$ -(1el)₂ conformation.

Thus, from the viewpoint of asymmetric transformation, the β -carbonyl carbon in the side chain of the amino acidate results

in a striking improvement in the chiral selectivity of the α -amino acidate.⁴ These results suggest the importance of intramolecular interligand hydrogen bonding. In previous papers, we have obtained considerable selectivities in some complexes, which were considered to be due mostly to interligand nonbonded repulsions.^{1,4} Such steric repulsions, however, cause not only selectivity but also destabilization of the system. In fact, the recovery of the alaninato complex, which showed high selectivity, was about 50%. On the contrary, the recovery of aspartato and asparaginato complexes was satisfactory, because an attractive force such as hydrogen bonding causes stabilization. The high stereoselectivity brought about through the interligand hydrogen bonding seems to be observed only in the complex having the appropriate structure with respect to the (N₄) part. Furthermore, the fact that only the aspartato and asparaginato complexes showed high chiral selectivities is thought to be a kind of substrate specificity, which is of interest in connection with enzyme systems.

Contribution from the Department of Chemistry, University of California, Davis, California 95616

X-ray Crystallographic Characterization of an Iron Porphyrin with a Vinylidene Carbene Inserted into an Iron-Nitrogen Bond

MARILYN M. OLMSTEAD, RU-JEN CHENG, and ALAN L. BALCH*

Received February 3, 1982

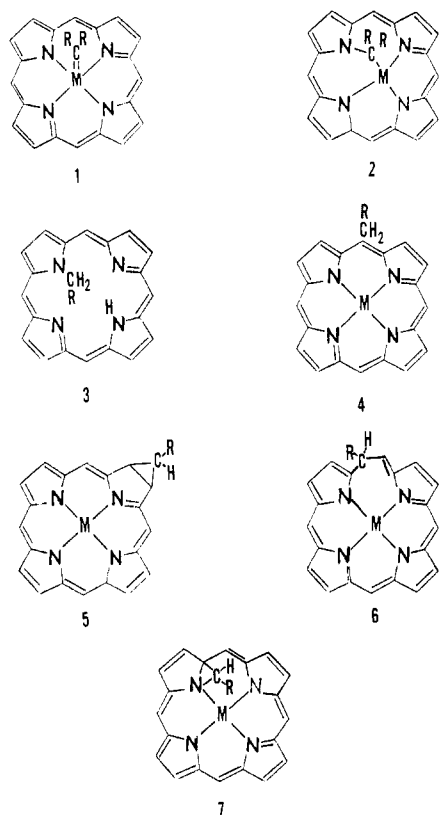
The complex TpTP[(*p*-ClC₆H₄)₂C=C]FeCl₂·2CH₂Cl₂, where TpTP is the dianion of *meso*-tetra-*p*-tolylporphyrin, has been characterized by single-crystal X-ray structural analysis. The compound crystallizes in the space group $P2_1/n$ with cell dimensions (140 K) of $a = 19.653$ (5) Å, $b = 12.418$ (2) Å, $c = 23.473$ (5) Å, and $\beta = 103.10$ (2)°. The structure was refined by blocked-cascade least-squares methods to a final R of 0.061 for the 6106 reflections which had $I > 3\sigma(I)$. The vinylidene carbene ligand has inserted into an iron-nitrogen bond. The iron atom is five-coordinate with approximate trigonal-bipyramidal geometry. Its donor set consists of three of the four porphyrin nitrogen atoms, the carbene atom, and the chlorine atom.

Introduction

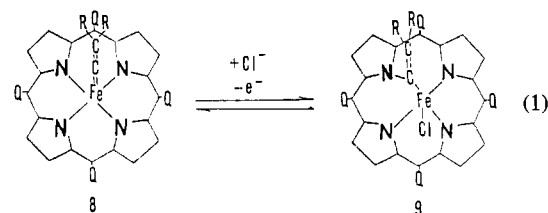
The reactions of potential carbene sources with metalloporphyrins have led to the synthesis of a variety of substances in which a R₂C fragment has been added to various portions of metalloporphyrin. A number of iron porphyrins with axial

carbene ligands, **1**, are known¹⁻³ and one of these, (TPP)Fe(CCl₂)H₂O, (TPP is the dianion of *meso*-tetraphenyl-

(1) Mansuy, D.; Lange, M.; Chottard, J. C.; Bartoli, J. F.; Chevrier, B.; Weiss, R. *Angew. Chem., Int. Ed. Engl.* **1978**, *17*, 781.



porphyrin) has been structurally characterized.¹ Another group of complexes, **2**, have an R_2C unit inserted into a metal–nitrogen bond.^{4–8} Other products derived from the addition of ethyl diazoacetate to metalloporphyrins include *N*-alkylporphyrins, **3**, and their metal complexes,⁹ meso-substituted porphyrins, **4**,^{10,11} cyclopropane chlorins, **5**,¹⁰ homoporphyrins, **6**,^{11,12} and an aziridine, **7**¹² (M = metal dication, $R = CO_2C_2H_5$ for **5–7**). The interconversion of some of these species has been observed. Thus treatment of the *N*-alkylated porphyrin **3** derived from *meso*-tetraphenylporphyrin with nickel acetylacetonate and nickel carbonate produced the homoporphyrin **6**.¹¹ Evidence exists that the aziridine, **7**, is an intermediate in this process.¹² Similarly, treatment of **3** derived from octaethylporphyrin with the nickel acetylacetonate/nickel carbonate mixture gave the meso-substituted porphyrin **4**.¹¹ We¹³ and Mansuy, Weiss, and co-workers¹⁴ have recently reported on another carbene migration reaction. In this reversible reaction, which is shown in eq 1 ($R = p\text{-ClC}_6\text{H}_4$, $Q = p\text{-CH}_3\text{C}_6\text{H}_4$), the vinylidene carbene complex **8**, obtained by Mansuy and co-workers² from iron(II) por-



phyrin chloride, iron powder, and 1,1-bis(*p*-chlorophenyl)-2,2,2-trichloroethene (DDT), undergoes oxidation by copper(II) halides or halogens to form **9**.¹⁵ The oxidation is accompanied by insertion of the carbene into an iron–nitrogen bond. The reaction may be reversed by treatment with sodium dithionite. Compound **8** is diamagnetic, and ¹H NMR observations indicate that it has the normal fourfold symmetry of a typical porphyrin complex. Consequently, it probably has a geometric structure similar to that of $(\text{TPP})\text{Fe}(\text{CCl}_2)\text{H}_2\text{O}$. On the other hand, **9** is paramagnetic with magnetic susceptibility and ESR spectrum that are consistent with an $S = 3/2$ ground state. The ¹H NMR spectrum of **9** indicates that it has only twofold or bilateral symmetry. Here we report on the details of an X-ray crystallographic study of **9**. Our results appear to be in essential agreement with the preliminary report of crystallographic data obtained for a different solvated form of this compound.¹⁴

Experimental Section

Crystals of **9** were prepared by diffusion of heptane into a dichloromethane solution contained in a thin tube. Although well-formed crystals were produced by this method, the majority of them yielded either broad or split peaks on an ω scan. The crystal selected for data collection was the only one examined that had sharp, single peaks on an ω scan; the average width at half-height was 0.37°. A summary of the important crystallographic data is given in Table I. The determination of cell constants and data collection were carried out on a Syntex P₂ diffractometer equipped with a Mo tube, graphite monochromator, and low-temperature apparatus. Final cell dimensions were obtained from a least-squares fit of 24 centered reflections with $30^\circ < 2\theta < 39^\circ$. The computed volume was 5579 (2) Å³. With allowance for the usual shrinkage at low temperature, this agrees well with the room-temperature density of 1.35 g cm⁻³, determined by flotation. The space group $P2_1/n$ (alternate setting of $P2_1/c$) was determined unambiguously from quick scans and the observation of systematic absences: $0k0, k$ odd; $h0l, h + l$ odd. Intensity data were obtained at 140 K with use of the parameters given in Table I. Reduction of intensity data to F_0 and $\sigma(F_0)$ was carried out as previously reported.¹⁶ The data were corrected for Lorentz and polarization effects but not for absorption.

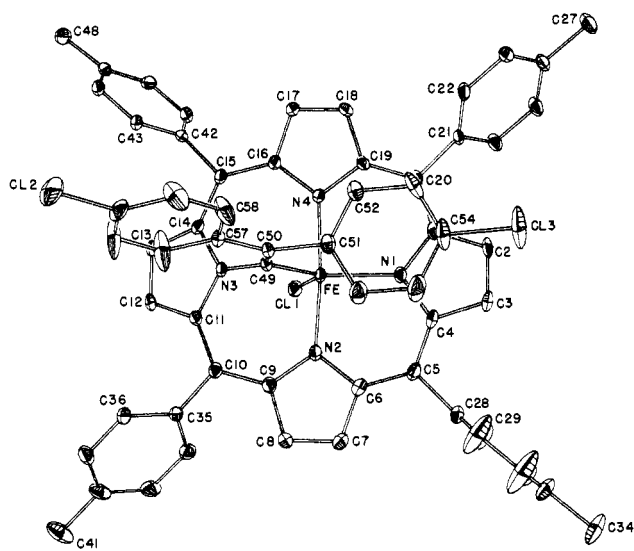
The positions of the iron atom and the three chlorine atoms were determined by direct methods. The remaining non-hydrogen atoms of the molecule were located in a subsequent Fourier map. After full-matrix least-squares refinement of these atoms, a difference map showed the presence of two partially disordered molecules of dichloromethane. Each of these had one ordered and one disordered chlorine atom. The disordered chlorine atoms exhibit approximately half-occupancy of two sites, 1.01 Å apart in one molecule and 1.55 Å apart in the other. With the inclusion of these two solvate molecules and isotropic thermal parameters, an R of 0.145 was obtained. Blocked-cascade least-squares refinement with anisotropic thermal parameters brought R to 0.061. During this latter refinement the site occupation factors for the two dichloromethane molecules were allowed to vary, and these converged with 84 and 93% occupancy for the two molecules. Hydrogen atoms were included with a model in which the computed hydrogen atom position is tied to the carbon atom positions being refined and the isotropic hydrogen thermal parameters are 1.2 times the equivalent isotropic thermal parameters of the corresponding carbon atom. There were a total of 705 least-squares parameters and 6106 unique observed reflections; the mean shift was

- (2) Mansuy, D.; Lang, M.; Chottard, J. C. *J. Am. Chem. Soc.* **1978**, *100*, 3214.
- (3) Mansuy, D.; Battioni, J.-P.; Chottard, J.-C.; Ullrich, V. *J. Am. Chem. Soc.* **1979**, *101*, 3571 and references therein.
- (4) Callot, H. J.; Tschamber, T.; Chevrier, B.; Weiss, R. *Angew. Chem., Int. Ed. Engl.* **1975**, *14*, 567.
- (5) Johnson, A. W.; Ward, D.; Batten, P.; Hamilton, A. L.; Shelton, G.; Elson, C. M. *J. Chem. Soc., Perkin Trans. 1* **1975**, 2076.
- (6) Johnson, A. W.; Ward, D. *J. Chem. Soc., Perkin Trans. 1* **1977**, 720.
- (7) Batten, P.; Hamilton, A. L.; Johnson, A. W.; Mahendram, M.; Ward, D.; King, T. J. *J. Chem. Soc., Perkin Trans. 1* **1977**, 1623.
- (8) Chevrier, B.; Weiss, R. *J. Am. Chem. Soc.* **1976**, *98*, 2985.
- (9) Callot, H. J.; Tschamber, T. *Bull. Soc. Chim. Fr.* **1973**, 3192.
- (10) Callot, H. J.; Johnson, A. W.; Sweeney, A. *J. Chem. Soc., Perkin Trans. 1* **1973**, 1424.
- (11) Callot, J. J.; Tschamber, T. *J. Am. Chem. Soc.* **1975**, *97*, 6175.
- (12) Callot, H. J.; Tschamber, T.; Schaeffer, E. *J. Am. Chem. Soc.* **1975**, *97*, 6178.
- (13) Latos-Grazynski, L.; Cheng, R.-J.; La Mar, G. N.; Balch, A. L. *J. Am. Chem. Soc.* **1981**, *103*, 4270.
- (14) Chevrier, B.; Weiss, R.; Lange, M.; Chottard, J.-C.; Mansuy, D. *J. Am. Chem. Soc.* **1981**, *103*, 2899.

- (15) Mansuy, D.; Lang, M.; Chottard, J.-C. *J. Am. Chem. Soc.* **1979**, *101*, 6437.
- (16) Balch, A. L.; Benner, L. S.; Olmstead, M. M. *Inorg. Chem.* **1979**, *18*, 2996.

Table I. Crystallographic Data for TpTP[(*p*-ClC₆H₄)₂C=C]FeCl·2CH₂Cl₂

fw	1177.14
<i>a</i> , Å	19.653 (5)
<i>b</i> , Å	12.418 (2)
<i>c</i> , Å	23.473 (5)
β, deg	103.10 (2)
<i>V</i> , Å ³	5579 (2)
<i>Z</i>	4
density, g cm ⁻³	1.35 (exptl) (298 K) 1.401 (calcd) (140 K)
cryst dimens, mm	0.20 × 0.40 × 0.50
cryst shape, color	prismatic, dark blue
space group	<i>P</i> 2 ₁ / <i>n</i> (alternate setting of <i>P</i> 2 ₁ / <i>c</i> , No. 14)
radiation	Mo Kα (λ = 0.710 69 Å)
temp, K	140
μ, cm ⁻¹	6.34
2θ _{max} , deg	45
scan speed, deg min ⁻¹	4–60
scan range, deg	1
scan type	ω
no. of unique data	7292
no. of data with <i>I</i> > 3σ(<i>I</i>)	6106

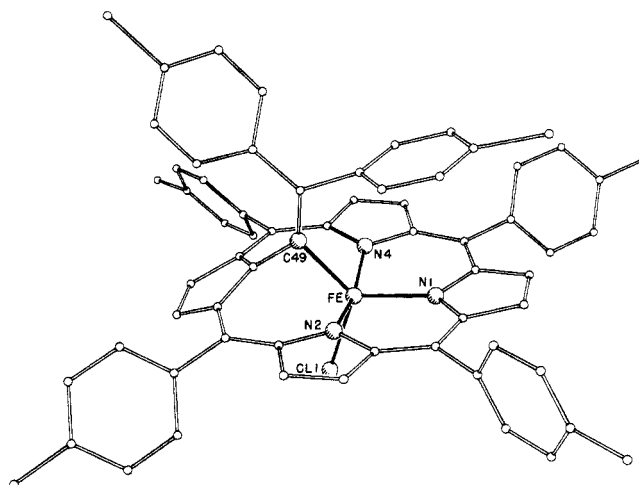
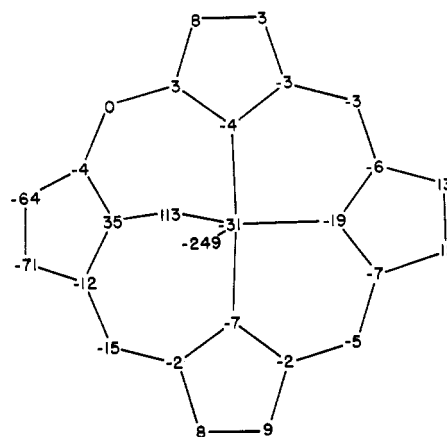
**Figure 1.** Perspective view of **9** showing the atom-labeling scheme.

less than 0.07 the maximum esd. Neutral-atom scattering factors^{17a} and corrections for anomalous scattering^{17b} were from ref 17. The quantity minimized during refinement was $\sum w(|F_o| - |F_c|)^2$, where $w = (1/\sigma^2(F_o))$. Solution and preliminary refinement of the structure were carried out with use of crystallographic programs developed by H. Hope and a CDC 7600 computer. Final refinement was carried out with use of the SHELXTL Revision 3 (July 1981) program library installed on a Data General Eclipse computer. The positional parameters and equivalent isotropic thermal parameters are listed in Table II. Anisotropic thermal parameters, hydrogen atom positions, and structure factor tables are available as supplementary material.

Results

A perspective drawing of **9**, which shows the atom-labeling scheme, is presented in Figure 1. A second view of the molecule is shown in Figure 2. Final atomic coordinates and thermal parameters are given in Table II. Selected interatomic distances and angles are presented in Tables III and IV. There are no interesting intermolecular contacts.

Coordination about Iron. The iron is bound to three of the porphyrin nitrogen atoms, the carbene carbon atom, and the chlorine atom. The fourth porphyrin nitrogen atom lies 2.529 (4) Å from the iron and is not directly bonded to it.

**Figure 2.** Another perspective view of **9**, which shows the tilt of the reacted pyrrole group from the plane of the rest of the porphyrin.**Figure 3.** Diagram of the porphyrin core in an orientation corresponding to Figure 1. Each atom symbol has been replaced by a number representing the perpendicular displacement, in units of 0.01 Å, from the mean plane of the porphyrin. This plane is based upon the location of the three unreacted pyrrole rings and the meso carbons connecting them.

The three Fe–N bond lengths, 2.002 (4), 1.991 (4), and 1.985 (4) Å, are similar. They are shorter than those found for high-spin ($S = 5/2$), five-coordinate iron(III) porphyrins,¹⁸ but they are similar in length to the Fe–N bonds of the intermediate-spin ($S = 3/2$), five-coordinate iron(III) complex (TPP)FeClO₄.¹⁹ On the other hand, the Fe–Cl bond length of 2.299 (1) Å is considerably longer than the corresponding distances in (TPP)FeCl (2.192 (12) Å)²⁰ and (protoporphyrin IX dimethyl ester)iron(III) chloride (2.218 (6) Å).²¹

The ligands about the iron atom form a distorted trigonal bipyramid. Two nitrogen atoms, N(2) and N(4), lie on the axis. The N(2)–Fe–N(4) bond angle is 164.5 (2)°. The equatorial ligand atoms N(1), C(49), and Cl(1) are nearly coplanar with the iron atom. This can be seen by inspection of Table V, which contains information about selected least-squares planes. The three angles between the equatorial ligands, 120.5, 111.7, and 127.8°, lie near the ideal value of 120°. The axial ligand–iron–equatorial ligand angles, 82.8, 83.1, 91.4, 92.2, 95.6, and 97.0°, cluster reasonably close to the ideal value of 90°.

(17) "International Tables for X-ray Crystallography"; Kynoch Press: Birmingham, England, 1974; Vol. 4: (a) pp 99–101; (b) pp 149–150.

(18) Scheidt, R. W. In "The Porphyrins"; Dolphin, D., Ed.; Academic Press: New York, 1978; Vol. 3, p 463.

(19) Reed, C. A.; Maskiko, T.; Bentley, S. P.; Kastner, M. E.; Scheidt, W. R.; Spertalian, K.; Lang, G. J. *Am. Chem. Soc.* **1979**, *101*, 2948.

(20) Hoard, J. L.; Cohen, G. H.; Glick, M. D. *J. Am. Chem. Soc.* **1967**, *89*, 1992.

(21) Koenig, D. F. *Acta Crystallogr.* **1976**, *18*, 663.

Table II. Atom Coordinates ($\times 10^4$) and Temperature Factors ($\text{Å}^2, \times 10^3$) for $\text{TpTP}[(p\text{-ClC}_6\text{H}_4)_2\text{C}=\text{C}]\text{FeCl}$

atom	x	y	z	U^a	atom	x	y	z	U^a
Fe	7206 (1)	57 (1)	4269 (1)	22 (1)	C(32)	5008 (4)	4374 (6)	3139 (3)	62 (3)
Cl(1)	8151 (1)	1071 (1)	4726 (1)	30 (1)	C(33)	5507 (3)	3617 (5)	3404 (3)	55 (2)
Cl(2)	5999 (1)	-5924 (1)	5808 (1)	67 (1)	C(34)	3792 (4)	4920 (7)	2654 (4)	101 (4)
Cl(3)	4836 (1)	-1109 (2)	2038 (1)	84 (1)	C(35)	6846 (3)	586 (4)	6281 (2)	25 (2)
N(1)	6769 (2)	633 (3)	3474 (2)	25 (1)	C(36)	6778 (3)	-149 (4)	6712 (2)	30 (2)
N(2)	6501 (2)	784 (3)	4625 (2)	26 (1)	C(37)	6810 (3)	194 (5)	7284 (5)	38 (2)
N(3)	7443 (2)	-1115 (3)	5174 (2)	24 (1)	C(38)	6905 (3)	1264 (5)	7434 (2)	42 (2)
N(4)	7754 (2)	-1015 (3)	3933 (2)	25 (1)	C(39)	6974 (3)	2002 (5)	7006 (2)	39 (2)
C(1)	6911 (3)	332 (4)	2952 (2)	26 (2)	C(40)	6945 (3)	1678 (4)	6441 (2)	33 (2)
C(2)	6434 (3)	859 (4)	2482 (2)	29 (2)	C(41)	6950 (3)	1646 (6)	8058 (3)	63 (3)
C(3)	6009 (3)	1473 (4)	2715 (2)	30 (2)	C(42)	8979 (3)	-2794 (4)	5058 (2)	27 (2)
C(4)	6213 (3)	1330 (4)	3343 (2)	27 (2)	C(43)	8868 (3)	-3706 (4)	5370 (2)	27 (2)
C(5)	5871 (3)	1765 (4)	3743 (2)	30 (2)	C(44)	9426 (3)	-4366 (4)	5627 (2)	30 (2)
C(6)	5992 (3)	1495 (4)	4336 (2)	29 (2)	C(45)	10101 (3)	-4116 (4)	5588 (2)	30 (2)
C(7)	5606 (3)	1900 (4)	4736 (2)	35 (2)	C(46)	10211 (3)	-3208 (4)	5275 (2)	30 (2)
C(8)	5878 (3)	1462 (4)	5262 (2)	31 (2)	C(47)	9657 (3)	-2553 (4)	5010 (2)	31 (2)
C(9)	6439 (3)	765 (4)	5201 (2)	27 (2)	C(48)	10706 (3)	-4804 (4)	5898 (2)	38 (2)
C(10)	6873 (2)	229 (4)	5683 (2)	25 (2)	C(49)	6930 (3)	-1187 (4)	4648 (2)	24 (2)
C(11)	7382 (3)	-541 (4)	5663 (2)	24 (2)	C(50)	6455 (3)	-1953 (4)	4483 (2)	26 (2)
C(12)	7988 (3)	-815 (4)	6105 (2)	29 (2)	C(51)	6017 (3)	-1813 (4)	3873 (2)	27 (2)
C(13)	8404 (3)	-1470 (4)	5869 (2)	27 (2)	C(52)	6231 (3)	-2254 (5)	3401 (2)	37 (2)
C(14)	8083 (3)	-1622 (4)	5266 (2)	26 (2)	C(53)	5851 (3)	-2044 (5)	2834 (2)	50 (2)
C(15)	8380 (3)	-2056 (4)	4827 (2)	25 (2)	C(54)	5276 (3)	-1399 (5)	2757 (2)	48 (2)
C(16)	8215 (3)	-1792 (4)	4225 (2)	26 (2)	C(55)	5057 (3)	-956 (6)	3213 (3)	51 (2)
C(17)	8550 (3)	-2304 (4)	3816 (2)	32 (2)	C(56)	5429 (3)	-1159 (5)	3774 (2)	39 (2)
C(18)	8307 (3)	-1842 (4)	3289 (2)	32 (2)	C(57)	6336 (3)	-2918 (4)	4821 (2)	27 (2)
C(19)	7806 (3)	-1046 (4)	3354 (2)	26 (2)	C(58)	5932 (4)	-3748 (5)	4554 (2)	54 (2)
C(20)	7415 (3)	-432 (4)	2892 (2)	26 (2)	C(59)	5816 (4)	-4670 (5)	4844 (3)	61 (3)
C(21)	7507 (3)	-632 (4)	2284 (2)	28 (2)	C(60)	6125 (3)	-4763 (4)	5425 (3)	39 (2)
C(22)	7364 (3)	-1629 (4)	2020 (2)	29 (2)	C(61)	6521 (4)	-3969 (6)	5700 (3)	82 (3)
C(23)	7397 (3)	-1794 (4)	1441 (2)	31 (2)	C(62)	6628 (4)	-3059 (6)	5408 (3)	83 (3)
C(24)	7579 (3)	-960 (4)	1112 (2)	33 (2)	C(63)	3676 (5)	2470 (8)	1103 (4)	74 (4)
C(26)	7730 (3)	39 (4)	1377 (2)	38 (2)	C(64)	-535 (4)	397 (7)	3928 (3)	66 (3)
C(26)	7698 (3)	200 (4)	1956 (2)	34 (2)	Cl(4)	276 (1)	-92 (2)	4317 (1)	71 (1)
C(27)	7598 (4)	-1131 (5)	478 (2)	47 (2)	Cl(5)	-575 (3)	496 (5)	3173 (2)	100 (2)
C(28)	5320 (3)	2586 (5)	3505 (2)	36 (2)	Cl(6)	-556 (4)	1199 (6)	3396 (3)	138 (4)
C(29)	4629 (3)	2321 (7)	3341 (4)	98 (4)	Cl(7)	3159 (1)	1321 (2)	1133 (1)	87 (1)
C(30)	4137 (4)	3060 (8)	3071 (5)	118 (5)	Cl(8)	4566 (2)	2303 (3)	1426 (2)	106 (2)
C(31)	4324 (3)	4092 (6)	2969 (3)	64 (3)	Cl(9)	4046 (5)	2777 (8)	1766 (4)	111 (4)

^a The equivalent isotropic U is defined as one-third of the trace of the orthogonalized U tensor.

The iron atom coordination in **9** can be compared to the iron atom coordination in chloro(*N*-methyl-*meso*-tetraphenylporphyrinato)iron(II) ($[\text{N-MeTPP}]\text{FeCl}$).²² In the latter compound the iron atom resides in a highly distorted, square-pyramidal environment with bonds to the four pyrrole nitrogen atoms and an axial chlorine atom. Alkylation affects the porphyrin in a fashion somewhat similar to that for the carbene insertion in that a substituent has added to the pyrrole nitrogen atoms. The Fe-Cl distance in $[\text{N-MeTPP}]\text{FeCl}$ is 2.244 (1) Å, somewhat shorter than found in **9**. In contrast the three strong Fe-N bonds in $[\text{N-MeTPP}]\text{FeCl}$ (Fe-N distances: 2.118 (2), 2.116 (2), 2.082 (2) Å) are all longer than the Fe-N bonds in **9** as is expected for the lower oxidation state of iron. In $[\text{N-MeTPP}]\text{FeCl}$ the iron atom coordination is completed by weak bonding to the alkylated pyrrole nitrogen at a distance of 2.329 (2) Å.

The Porphyrin. Due to the insertion of the carbene into the iron-nitrogen bond, the porphyrin is no longer planar. The pyrrole to which the carbene has been added is sharply angled out of the plane of the rest of the porphyrin. This can be seen in the perspective view in Figure 2 and in another form in Figure 3. Figure 3 shows the deviations of the atoms in the porphyrin skeleton from a least-squares plane calculated on the basis of the three unreacted pyrrole rings. The iron atom lies near this plane while the reacted pyrrole is tilted so that N(3) lies on the opposite side of the plane from the iron atom.

Nevertheless, this pyrrole ring has retained its planarity, although the adjacent meso carbons are significantly displaced from its plane. The carbene carbon, however, does lie close to the plane of the pyrrole. The dihedral angle between the plane containing the reacted pyrrole and the plane of the rest of the porphyrin is 28°. Similar distortions are shown by complexes containing a carbene or a nitrene inserted into a metal-nitrogen bond of a porphyrin²³ and by *N*-alkylated porphyrins.²⁴⁻²⁷

The carbene insertion does not appear to have appreciably altered the π delocalization as measured by the bond lengths. With C_α , C_β , and C_m representing the pyrrole carbon atoms adjacent to nitrogen atoms, the pyrrole carbon atoms remote from the nitrogen atoms, and the meso carbon atoms, respectively, strain-free distances in the porphyrin are expected to be as follows: C_α - C_β , 1.355; C_α - C_m , 1.395; N - C_α , 1.384 Å.²⁸ Inspection of Table II shows that in **9** there are no unusual variations from these ideal values for any portion of the porphyrin. Comparison of the structural data for complexes with carbene insertion into the porphyrin-metal bond and data for metal complexes of *N*-alkylated porphyrins re-

(22) Anderson, G. P.; Kopelove, A. B.; Lavalley, D. K. *Inorg. Chem.* **1980**, *19*, 2101.

(23) Callot, H. J.; Chevrier, B.; Weiss, R. *J. Am. Chem. Soc.* **1978**, *100*, 4733.

(24) Goldberg, D. E.; Thomas, K. M. *J. Am. Chem. Soc.* **1976**, *98*, 913.

(25) Anderson, O. P.; Lavalley, D. K. *J. Am. Chem. Soc.* **1977**, *99*, 1404.

(26) Anderson, O. P.; Lavalley, D. K. *Inorg. Chem.* **1977**, *16*, 1634.

(27) Lavalley, D. K.; Kopelove, A. B.; Anderson, O. P. *J. Am. Chem. Soc.* **1978**, *100*, 3025.

(28) Hoard, J. L. *Ann. N.Y. Acad. Sci.* **1973**, *206*, 18.

Table III. Bond Lengths (Å) for TpTP[(*p*-ClC₆H₄)₂C=C]FeCl

Fe-N(1)	2.002 (4)	Fe-N(2)	1.991 (4)
Fe-Cl(1)	2.299 (1)	Fe-N(4)	1.985 (4)
Fe-C(49)	1.921 (5)	Cl(2)-C(60)	1.746 (6)
Cl(3)-C(54)	1.750 (5)	N(1)-C(1)	1.368 (6)
N(1)-C(4)	1.374 (6)	N(2)-C(6)	1.391 (6)
N(2)-C(9)	1.382 (6)	N(3)-C(11)	1.379 (6)
N(3)-C(14)	1.379 (6)	N(3)-C(49)	1.409 (5)
N(4)-C(16)	1.393 (6)	N(4)-C(19)	1.386 (6)
C(1)-C(2)	1.434 (6)	C(1)-C(20)	1.401 (7)
C(2)-C(3)	1.338 (8)	C(3)-C(4)	1.448 (7)
C(4)-C(5)	1.382 (8)	C(5)-C(6)	1.398 (7)
C(5)-C(28)	1.499 (7)	C(6)-C(7)	1.426 (8)
C(7)-C(8)	1.344 (7)	C(8)-C(9)	1.434 (7)
C(9)-C(10)	1.418 (6)	C(10)-C(11)	1.393 (7)
C(10)-C(35)	1.485 (7)	C(11)-C(12)	1.432 (6)
C(12)-C(13)	1.358 (7)	C(13)-C(14)	1.427 (6)
C(14)-C(15)	1.400 (7)	C(15)-C(16)	1.416 (6)
C(15)-C(42)	1.493 (7)	C(16)-C(17)	1.430 (8)
C(17)-C(18)	1.348 (7)	C(18)-C(19)	1.429 (7)
C(19)-C(20)	1.403 (6)	C(20)-C(21)	1.499 (7)
C(21)-C(22)	1.385 (7)	C(21)-C(26)	1.390 (7)
C(22)-C(23)	1.390 (7)	C(23)-C(24)	1.385 (8)
C(24)-C(25)	1.388 (7)	C(24)-C(27)	1.514 (7)
C(25)-C(26)	1.391 (7)	C(28)-C(29)	1.365 (8)
C(28)-C(33)	1.367 (9)	C(29)-C(30)	1.379 (12)
C(30)-C(31)	1.368 (12)	C(31)-C(32)	1.358 (9)
C(31)-C(34)	1.532 (11)	C(32)-C(33)	1.399 (9)
C(35)-C(36)	1.391 (7)	C(35)-C(40)	1.409 (7)
C(36)-C(39)	1.395 (7)	C(37)-C(39)	1.378 (9)
C(38)-C(39)	1.389 (8)	C(38)-C(41)	1.523 (8)
C(39)-C(40)	1.375 (8)	C(42)-C(43)	1.392 (7)
C(42)-C(47)	1.395 (8)	C(43)-C(44)	1.393 (7)
C(44)-C(45)	1.386 (8)	C(45)-C(46)	1.388 (7)
C(45)-C(48)	1.510 (7)	C(45)-C(47)	1.389 (7)
C(49)-C(50)	1.327 (7)	C(50)-C(51)	1.505 (6)
C(50)-C(57)	1.484 (7)	C(51)-C(52)	1.384 (8)
C(51)-C(56)	1.387 (7)	C(52)-C(53)	1.396 (7)
C(53)-C(54)	1.364 (9)	C(54)-C(55)	1.358 (9)
C(55)-C(56)	1.377 (7)	C(57)-C(58)	1.364 (8)
C(57)-C(62)	1.380 (7)	C(58)-C(59)	1.377 (9)
C(59)-C(60)	1.366 (8)	C(60)-C(61)	1.329 (9)
C(61)-C(62)	1.363 (10)	C(63)-Cl(7)	1.762 (10)
C(63)-Cl(8)	1.753 (9)	C(63)-Cl(9)	1.608 (12)
C(64)-Cl(4)	1.757 (7)	C(64)-Cl(5)	1.762 (9)
C(64)-Cl(6)	1.590 (11)		

veals that N-alkylation produces more striking changes in the porphyrin skeleton distances.

The Carbene. The terminal carbon atom of the carbene is clearly inserted into the iron-nitrogen bond so that it is attached to N(3) and the iron atom. The unit comprised of N(3), C(49), Fe, C(50), C(58), and C(51) is nearly planar as expected for atoms surrounding the C(49)-C(50) double bond. The C(49)-C(50) bond length, 1.327 (7) Å, is reasonable for a carbon-carbon double bond. One of the phenyl rings attached to the double bond is nearly coplanar with it. The angle between the plane of the phenyl ring containing C(57) and the plane of the carbene double bond is 11.8°. The other phenyl ring is nearly perpendicular to the double bond with an angle between the plane of the phenyl group containing C(51) and the plane of the double bond of 86.8°.

Discussion

Despite the difficulties we have had obtaining a suitable crystal of **9** or of its *meso*-tetraphenylporphyrin analogue, the one useful crystal that we found does appear to be representative of the bulk sample. The structure found crystallographically is fully in accord with the structural information available from extensive ¹H and ¹³C NMR studies of **9** and its analogues.^{13,29}

Table IV. Bond Angles (Deg) for TpTP[(*p*-ClC₆H₄)₂C=C]FeCl

N(1)-Fe-N(2)	92.2 (2)	N(1)-Fe-Cl(1)	111.7 (1)
N(2)-Fe-Cl(1)	97.0 (1)	N(1)-Fe-N(4)	91.4 (2)
N(2)-Fe-N(4)	164.5 (2)	Cl(1)-Fe-N(4)	95.6 (1)
N(1)-Fe-C(49)	127.8 (2)	N(2)-Fe-C(49)	82.8 (2)
Cl(1)-Fe-C(49)	120.5 (1)	N(4)-Fe-C(49)	83.1 (2)
Fe-N(1)-C(1)	127.3 (3)	Fe-N(1)-C(4)	125.7 (3)
C(1)-N(1)-C(4)	106.6 (4)	Fe-N(2)-C(6)	125.0 (3)
Fe-N(2)-C(9)	128.8 (3)	C(6)-N(2)-C(9)	106.1 (4)
C(11)-N(3)-C(14)	110.7 (4)	C(11)-N(3)-C(49)	125.6 (4)
C(14)-N(3)-C(49)	123.6 (4)	Fe-N(4)-C(16)	128.3 (3)
Fe-N(4)-C(19)	125.1 (3)	C(16)-N(4)-C(19)	106.2 (4)
N(1)-C(1)-C(2)	109.5 (4)	N(1)-C(1)-C(20)	124.5 (4)
C(2)-C(1)-C(20)	125.9 (4)	C(1)-C(2)-C(3)	107.8 (4)
C(2)-C(3)-C(4)	107.0 (4)	N(1)-C(4)-C(3)	109.1 (4)
N(1)-C(4)-C(5)	125.5 (4)	C(3)-C(4)-C(5)	125.3 (4)
C(4)-C(5)-C(6)	125.6 (5)	C(4)-C(5)-C(28)	115.7 (4)
C(6)-C(5)-C(28)	118.7 (5)	N(2)-C(6)-C(5)	125.6 (5)
N(2)-C(6)-C(7)	109.4 (4)	C(5)-C(6)-C(7)	125.1 (5)
C(6)-C(7)-C(8)	107.5 (5)	C(7)-C(8)-C(9)	108.0 (5)
N(2)-C(9)-C(8)	109.0 (4)	N(2)-C(9)-C(10)	128.1 (5)
C(8)-C(9)-C(10)	122.7 (5)	C(9)-C(10)-C(11)	127.0 (5)
C(9)-C(10)-C(35)	118.1 (4)	C(11)-C(10)-C(35)	114.6 (4)
N(3)-C(11)-C(10)	125.5 (4)	N(3)-C(11)-C(12)	105.5 (4)
C(10)-C(11)-C(12)	128.6 (4)	C(11)-C(12)-C(13)	108.9 (4)
C(12)-C(13)-C(14)	108.2 (4)	N(3)-C(14)-C(13)	106.1 (4)
N(3)-C(14)-C(15)	125.3 (4)	C(13)-C(14)-C(15)	128.1 (4)
C(14)-C(15)-C(16)	127.3 (4)	C(14)-C(15)-C(42)	113.2 (4)
C(16)-C(15)-C(42)	119.2 (4)	N(4)-C(16)-C(15)	128.9 (5)
N(4)-C(16)-C(17)	109.0 (4)	C(15)-C(16)-C(17)	122.0 (4)
C(16)-C(17)-C(18)	107.7 (5)	C(17)-C(18)-C(19)	107.9 (5)
N(4)-C(19)-C(18)	109.2 (4)	N(4)-C(19)-C(20)	126.4 (5)
C(18)-C(19)-C(20)	124.4 (5)	C(1)-C(20)-C(19)	124.5 (5)
C(1)-C(20)-C(21)	116.6 (4)	C(19)-C(20)-C(21)	118.9 (4)
C(20)-C(21)-C(22)	121.2 (5)	C(20)-C(21)-C(26)	120.7 (4)
C(22)-C(21)-C(26)	118.0 (4)	C(21)-C(22)-C(23)	121.3 (5)
C(22)-C(23)-C(24)	120.6 (5)	C(23)-C(24)-C(25)	118.3 (5)
C(23)-C(24)-C(27)	120.7 (5)	C(25)-C(24)-C(27)	121.0 (5)
C(24)-C(25)-C(26)	120.9 (5)	C(21)-C(26)-C(25)	120.8 (5)
C(5)-C(28)-C(29)	122.0 (6)	C(5)-C(28)-C(33)	120.1 (5)
C(29)-C(28)-C(33)	117.8 (6)	C(28)-C(29)-C(30)	121.2 (8)
C(29)-C(30)-C(31)	121.0 (7)	C(30)-C(31)-C(32)	118.5 (7)
C(30)-C(31)-C(34)	122.1 (6)	C(32)-C(31)-C(34)	119.3 (7)
C(31)-C(32)-C(33)	120.3 (7)	C(28)-C(33)-C(32)	121.1 (6)
C(10)-C(35)-C(36)	121.5 (4)	C(10)-C(35)-C(40)	120.4 (5)
C(36)-C(35)-C(40)	117.9 (5)	C(35)-C(36)-C(37)	120.6 (5)
C(36)-C(37)-C(38)	121.0 (5)	C(37)-C(38)-C(39)	118.7 (5)
C(37)-C(38)-C(41)	121.5 (5)	C(39)-C(38)-C(41)	119.8 (6)
C(38)-C(39)-C(40)	121.0 (5)	C(35)-C(40)-C(39)	120.8 (5)
C(15)-C(42)-C(43)	119.1 (5)	C(15)-C(42)-C(47)	121.8 (4)
C(43)-C(42)-C(47)	118.9 (4)	C(42)-C(43)-C(44)	120.3 (5)
C(43)-C(44)-C(45)	120.7 (5)	C(44)-C(43)-C(46)	118.9 (5)
C(44)-C(45)-C(48)	120.1 (5)	C(46)-C(45)-C(48)	120.0 (5)
C(45)-C(46)-C(47)	120.9 (5)	C(42)-C(47)-C(46)	121.3 (5)
Fe-C(49)-N(3)	97.7 (3)	Fe-C(49)-C(50)	134.0 (3)
N(3)-C(49)-C(50)	128.2 (4)	C(49)-C(50)-C(51)	114.1 (4)
C(49)-C(50)-C(57)	127.5 (4)	C(51)-C(50)-C(57)	118.4 (4)
C(50)-C(51)-C(52)	120.2 (4)	C(50)-C(51)-C(56)	120.2 (5)
C(52)-C(51)-C(56)	119.4 (4)	C(51)-C(52)-C(53)	119.7 (5)
C(52)-C(53)-C(54)	119.0 (5)	Cl(3)-C(54)-C(53)	117.6 (4)
Cl(3)-C(54)-C(55)	120.1 (5)	C(53)-C(54)-C(55)	122.3 (5)
C(54)-C(55)-C(56)	119.0 (6)	C(51)-C(56)-C(55)	120.6 (5)
C(50)-C(57)-C(58)	120.8 (4)	C(50)-C(57)-C(62)	123.7 (5)
C(58)-C(57)-C(62)	115.5 (5)	C(57)-C(58)-C(59)	123.1 (5)
C(58)-C(59)-C(60)	118.6 (6)	Cl(2)-C(60)-C(59)	120.1 (4)
Cl(2)-C(60)-C(61)	119.9 (5)	C(59)-C(60)-C(61)	120.0 (6)
C(60)-C(61)-C(62)	120.8 (6)	C(57)-C(62)-C(61)	122.0 (6)
Cl(7)-C(63)-Cl(8)	114.5 (5)	Cl(7)-C(63)-Cl(9)	107.0 (7)
Cl(8)-C(63)-Cl(9)	54.6 (5)	Cl(4)-C(64)-Cl(5)	112.0 (5)
Cl(4)-C(64)-Cl(6)	118.9 (6)	Cl(5)-C(64)-Cl(6)	34.8 (4)
C(64)-Cl(5)-Cl(6)	63.3 (5)	C(64)-Cl(6)-Cl(5)	81.9 (6)
C(63)-Cl(8)-Cl(9)	57.9 (5)	C(63)-Cl(9)-Cl(8)	67.5 (5)

The determination of the correct structure for **9** combined with the known reversible redox chemistry of this species establishes the interconversion shown in eq 1. This has further implications for the nature of the reactive forms of heme proteins bearing oxo ligands.

(29) Latos-Grazynski, L.; Cheng, R. J.; La Mar, G. N.; Balch, A. L., to be submitted for publication.

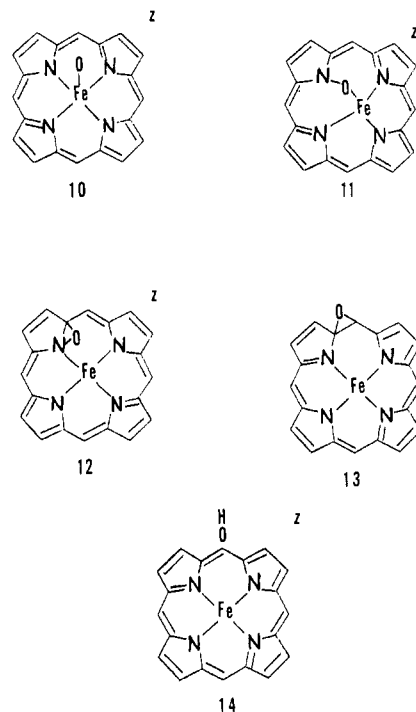
Table V. Selected Least-Squares Planes in 9^a

atom	dev from plane, Å	atom	dev from plane, Å
Plane 1: $14.0152x - 7.1502y - 12.9373z = 4.5908$			
Fe	-0.006	C(49)	0.008
N(1)	-0.002	N(3)	-0.005
Cl(1)	0.004		
Plane 2: $10.0207x + 9.9898y - 9.6802z = 1.3174$			
N(3)	0.019	C(12)	-0.037
C(49)	-0.058	C(13)	-0.046
C(14)	0.065	C(10) ^b	0.297
C(11)	0.058	C(15) ^b	0.354
Plane 3: $12.5430x + 9.5307y - 2.0109z = 8.3919$			
N(1)	0.003	C(3)	0.003
C(1)	-0.001	C(4)	-0.004
C(2)	-0.001		
Plane 4: $11.9918x + 9.4562y + 1.7553z = 9.3549$			
N(2)	-0.006	C(8)	0.000
C(6)	0.006	C(9)	0.003
C(7)	-0.004		
Plane 5: $14.8134x - 6.6818y - 12.6372z = 5.2223$			
Fe	0.018	N(3)	0.010
C(57)	0.021	C(50)	-0.021
C(49)	-0.037	C(51)	0.008

^a The errors associated with the deviations from the least-squares planes are 0.001 Å for Fe, 0.002 Å for Cl(1), and 0.005 Å for carbon and nitrogen atoms. ^b These atoms were not part of the calculation determining the least-squares plane.

The recognition of the considerable formal similarities between the oxygen atom transfer reactions catalyzed by mixed function oxidases such as cytochrome P-450 and the reactions of carbenes led to the development of an oxenoid mechanism of action for these enzymes. (An oxygen atom (oxene) and a carbene are isoelectronic.³⁰) Moreover, it was noted that amine oxides under photochemical activation could mimic some of the same transformations that cytochrome P-450 catalyzes.³¹ An alternate view of these reactions noted the similarity of their nature to that of the reactions of metal oxo complexes.³² Our structural studies suggest that the metal oxo species **10** and structure **11** may be closely linked.¹³ The mechanisms of action of cytochrome P-450 and the peroxidases are both believed to pass through a stage where a complex of the stoichiometry (P)FeO⁺ (P = porphyrin dianion) is present.^{33,34} These intermediates have different reactivities, which may be related to the structural location of the oxygen atom. Thus the reactive form of cytochrome P-450 may possess structure **11**. This structure is obviously related to porphyrin N-oxides, and investigations of porphyrin N-oxides indicate that these readily lose their oxygen atom. Because of this aspect of their reactivity, Bonnett et al. have also, independently, suggested that a complex with structure **11** may be involved in the action of cytochrome P-450.³⁵

The position of the carbene ligand in reaction 1 is linked to a redox process. The location of the oxygen atom between



10 and **11** may similarly be linked to oxidation level or it may be controlled by the presence or absence of a proton. Thus the difference in reactivity of cytochrome P-450 and peroxidase intermediates may be determined by the availability of protons at the active sites of these proteins.

The mobility of a carbene-derived moiety in porphyrin complexes is not limited to transfer from metal into the metal-nitrogen bond but extends to link structures **3**, **4**, and **7**. Parallel behavior for a metal oxo unit can account for porphyrin meso hydroxylation, which occurs in heme oxidase³⁶ and in the reaction of peroxide with certain metal porphyrins.³⁷ Heme oxidase is responsible for heme catabolism with the eventual formation of free iron ion, carbon monoxide, and bilirubin. Heme functions as both cofactor and substrate, and an iron oxyphlorin is an intermediate. While details of the mechanism of hydroxylation are incomplete, an oxygenated form of the heme/heme oxidase complex has been detected. The formation of a ferryl complex **10** followed by oxygen atom migration through structures **11**, **12**, and **13** to **14** could account for the hydroxylation reaction. Similarly the reaction of peroxide with metal porphyrins can produce an oxyphlorin, but the success of this reaction is dependent on the metal, its oxidation state, and axial ligation. This sensitivity to the metal suggests the oxygen introduction may begin at the metal with oxene migrations following.

Acknowledgment. We thank the National Institutes of Health (Grant No. GM 26226) for support.

Registry No. **8**, 77742-80-4; **9**, 83174-86-1.

Supplementary Material Available: Tables of structure factors for TpTP[(p-ClC₆H₄)₂C=C]FeCl, anisotropic thermal parameters (Table VI), and hydrogen coordinates (Table VII) (41 pages). Ordering information is given on any current masthead page.

- (30) Hamilton, G. A. In "Molecular Mechanisms of Oxygen Activation"; Hayaishi, O., Ed.; Academic Press: New York, 1974; p 405.
 (31) Jerina, D. M.; Boyd, D. R.; Daly, J. W. *Tetrahedron Lett.* **1970**, 457.
 (32) Sharpless, K. B.; Flood, T. C. *J. Am. Chem. Soc.* **1971**, *93*, 2316.
 (33) Hewson, W. D.; Hager, L. P. In "The Porphyrins"; Dolphin, D., Ed.; Academic Press: New York, 1979; p 295.
 (34) Griffin, B. W.; Peterson, J. A.; Estabrook, R. W. In "The Porphyrins"; Dolphin, D., Ed.; Academic Press: New York, 1979; p 333.
 (35) Bonnett, R.; Ridge, R. J.; Appleman, E. H. *J. Chem. Soc., Chem. Commun.* **1979**, 310.

- (36) Yoshida, T.; Noguchi, M.; Kikuchi, G. *J. Biol. Chem.* **1980**, *255*, 4418 and references therein.
 (37) Bonnett, R.; Dimsdale, M. J. *J. Chem. Soc., Perkin Trans.* **1972**, 2540.